# Zone-Based Multiple Regression Models to Visualize GPS Locations in a Network Camera Image

Daniel James Moore

Thesis submitted to the faculty of the Virginia Polytechnic Institute and State University in partial fulfillment of the requirements for the degree of

Master of Science
In
Geography

Laurence W. Carstensen, Chair
Peter M. Sforza
James B. Campbell

May 6, 2015
Blacksburg, VA

Keywords: GPS, public safety, mobile phones, regression, surveillance

# Zone-Based Multiple Regression Models to Visualize GPS Locations in a Network Camera Image

Daniel Moore

## ABSTRACT

Surveillance cameras are integral in assisting law enforcement by collecting video information that may help officers detect people for whom they are looking. While surveillance cameras record the area covered by the camera, unlike humans, they cannot "understand" what is happening. My research uses multiple curvilinear regression models to accurately place differentially corrected GPS points with submeter accuracy onto a camera image. Optimal results were achieved after splitting the image into four zones with the focus on calibrating each area separately. This resulted in adjusted $R^2$ values as high as 99.8 percent, indicating that high quality GPS points can form a good manual camera calibration. To ascertain whether or not a lesser quality GPS point associated with a social media application would allow location of the person sending the message, I used an iPhone 5s to do a follow up. Using the zone-based calibration equations on GPS point locations from an iPhone 5s show that the locations collected are less accurate than differentially corrected GPS locations, but there is still a decent chance of being able to locate the correct person in an image based off that person's location. That chance, however, depends on the population density inside the image. Pedestrian density tests show that about 70-80 percent of the phone locations in a low-density environment could be used to locate the correct person that sent a message while 30-60 percent of the phone locations could be used in that manner in a high-density environment.

# Table of Contents

# Figures

# Tables

## 1. Introduction

As smartphones with GPS capabilities have become more readily available and affordable, use of a smartphone's GPS location has become more common. Although GPS locations collected from mobile phones are helpful to certain vertical markets, this research focuses on governmental applications, specifically public safety. Accurate location derived from a phone call may be the deciding factor between life and death in an emergency. The Federal Communications Commission estimates that, as of December 2014, 70% of 911 calls originate from wireless phones (Federal Communications Commission 2014). Current Enhanced 911 (E911) Public Safety Answering Points (PSAPs) can collect accurate locations from a landline, but it is more difficult to get an accurate location from a mobile phone (Federal Communications Commission 2014). The FCC's E911 wireless services' Phase II rules state that wireless service providers should be able to provide accurate enough data (Latitude and Longitude) to locate the caller within 50 to 300 meters (Federal Communications Commission 2014). At this time, not all location information from wireless phones is provided with "Phase II" accuracy. Find Me 911, "A coalition to ensure that 911 works in today's wireless age"(2014), found that 9 of every 10 wireless calls to 911 in Washington, D.C from December 2012 to July 2013 did not contain an accurate location. This locational information is vital in order "to find callers who are lost, confused, unconscious, or otherwise unable to share their location" (Find Me 911 2014).

The goal of this research is to determine if GPS points are accurate enough to locate someone on a camera. To do this, differentially corrected sub-meter GPS data was used to calibrate a camera to the geographic area used in this study. I hypothesize that, after running differentially corrected and smartphone GPS points through multiple-regression models

generated from manual camera calibration, I should be able to locate myself on a surveillance camera based on the time and location a GPS point was collected. By calibration, I mean the process of using differentially corrected GPS reference points inside the image from the camera and comparing those GPS points to their 2D coordinates in the image. This comparison was done in order to "detect, correlate, adjust, rectify, and document the accuracy" (Cable 2005, p. 1) of the models that were generated (Cable 2005). To generate a reliable system, the differentially corrected GPS points and smartphone GPS points need to be located within one meter of the intended location. Most mapping-grade GPS devices, like the one used in this calibration, have submeter accuracy once the points are differentially corrected. Points located over one meter away from their intended location would increase chances of not locating someone, or selecting the wrong person on an image.

In law enforcement, this idea could be helpful in locating suspects or persons of interest on an image. Depending on the resolution and placement of the camera, one could use the suspect's clothing to assist the location process. With higher resolution cameras (1080p or 4K/2160p) it is possible, depending on how close the camera is to the area being covered, that a suspect could be located and identified in a scene that was previously covered by a 720p or lower resolution camera. The image from the higher resolution camera would collect enough details on the person, once located, that could be used to identify that person in a database. If an upgrade to a higher resolution camera cannot "identify" someone in a specific scene, one would still be able to collect and use more attributes to locate that person. If one knows a suspect is wearing a yellow shirt, a higher resolution camera (1080p or above) could also bring out details on the shirt (logos, other colors, sleeves). Another attribute that could be collected is the height of the person. This measurement from a higher resolution camera would be more precise than a measurement

from a 720p camera. While this may raise concern for privacy, the applications that can come out of the process of placing a GPS point on an image could be beneficial. Products that cater to Law Enforcement, like AGSI's Go360™ Public Safety, utilization of tracking of publicly available Location-Based Social Network (LBSN) data and use that data against "any type of illegal activity including cyber-bullying, shootings and stabbings, drugs, public demonstrations, gang activity and organized crime"(AGSI 2015). This research, especially if it is implemented alongside a system like Go360™ Public Safety, would make locating a person on an image more efficient. A law enforcement operations center could collect location-based social network data by keywords, usernames, geographic area, and date and time, which could be processed through camera calibration algorithms calibrated to cameras in the area (AGSI 2015). If the geographic location on the LBSN data is accurate enough, one could pinpoint the person on the image based on information posted publicly on a social networking site.

Can mobile GPS data be visualized in that manner? Previous research addresses Cameras and their ability to "understand" their surroundings; mapping-grade and mobile GPS accuracy; Research related to uses of LBSN data; and, the recent implementation on Next Generation 911. These topics and themes build foundations for this research and identify topics where this research could move forward.

# 2. Literature Review

## 2A. Camera Calibration and the Ability to "Understand" Surroundings

Cameras record what is in front of them and research, including this study, attempts to create new ways in which cameras can "understand" what is in front of them. Even though cameras can record video and save it for later viewing, the process of watching and interpreting the video feed requires a human presence (Cetin et al. 2013). The overarching subject in this research is computer vision, which is "the science of endowing computers or other machines with vision, or the ability to see"(Learned-Miller 2011, p. 2).

This research was heavily influenced by the results and testing done in Charles Staton's (2013) project at Virginia Tech titled "Citizens as Sensors: Examining Tsai's Camera Algorithm Using a Location Based Social Network and Smartphone GPS Capabilities". Staton's (2013) research looked at the possibility of using Twitter's location data and processing it through Tsai's (1987) camera calibration algorithm to see if one can actually be located on an internet camera based on data passed along with a tweet they sent. A major issue with Staton's work was the inaccuracy of the Tsai algorithm for the camera used in the study. This study, however, takes a step back from Staton's (2013) study to see if a more accurate camera calibration model improves the locational accuracy of mapping-grade and smartphone GPS points. If camera calibration models are capable of doing this, then future research could re-examine the accuracy of LBSN Data and the possibility of seeing a given GPS location accurately on an image.

Another problem with collecting LBSN data is the time associated with a post. Since cameras record video at multiple frames per second, the exact time a social network post was made is critical in order to reference a tweet or social network post to the correct frame. Staton's study could only collect tweet times to the nearest minute, which is not a precise enough

measurement to use when locating someone on an image (Staton 2013, p. 19). Even though Staton had participants hold up a sign when each tweet was sent to make selecting camera time easier, the time lapse between the tweet time and the camera time could not be measured because of the lack of precision (Staton 2013). The Trimble® GPS used for this study logs to the second the time a signal was acquired collect a location, which makes time error easier to measure. Comparing each GPS location's timestamp to the timestamp on a camera could complete this task.

An automatic camera calibration algorithm like Tsai's (1987) requires a user to know extrinsic (rotations and 3D translation) and intrinsic (effective focal length, distortion coefficient, uncertainty scale factor, and image coordinate for the origin in the image plane) parameters about the camera in order to effectively use an automatic calibration model (Tsai 1987). For this study, there were two primary reasons that manual camera calibration was used. The first reason was that the goal entering the study was to see if using multiple regression models to calibrate a camera could be an effective and accurate method such that later points could be used to locate a person in an image. The second reason was that the intrinsic parameters from the camera, required to effectively use an automatic calibration model could not be retrieved. The manual calibration used in this study did not require a user to know details about a camera that were required to use in a model besides the image coordinates.

Tsai's Algorithm was designed for cameras with pinhole distortion (Tsai 1987), which is not the lens distortion present on the Axis P1354 camera used in Staton's (2013) study. The Axis P1354 is a High-Definition fixed network camera that streams video at 720p -HDTV resolution- at 25/30 frames per second depending on the frequency from the power line (Axis Communications 2014). Axis states that this camera performs well in both indoor and outdoor

environments and “is perfect for securing locations such as governmental and industrial buildings, retail stores, airports, railway stations, schools and university campuses”(Axis Communications 2014). Another difference between automatic and manual calibration is that automatic calibration models adjust to changes in camera geometry (refocus, change angle of view, etc.) without the need to recalibrate (Staton 2013). Manual camera calibration models, however, would need to be redeveloped any time the camera is adjusted (Hsien-Chou and Hong-Jhih 2009). Use of a manual camera calibration approach could help reduce Staton’s (2013) high residual errors, without requiring details of the camera’s intrinsic parameters.

Liao Hsien-Chou and Wu Hong-Jhih (2009) tracked a moving GPS point upon entrance into a camera frame and compared the residuals generated from both manual and automatic camera calibration algorithms. The goal is to see if automatic camera calibration can be used to set up their tracking and yield better results than a manual camera calibration. According to Hsien-Chou and Hong-Jhih (2009), manual camera calibration “is not only an inconvenient procedure, but also troublesome because the camera must be re-calibrat[ed] when it is moved slightly” (Hsien-Chou and Hong-Jhih 2009, p. 760). Hsien-Chao and Hong-Jhih can track the operator’s movement while carrying a GPS device when entering the image, but “the accuracy of calibration points generated by [an] automatic method is similar to that of manual calibration points”(Hsien-Chou and Hong-Jhih 2009, p. 763). Even though automatic camera calibration is less time consuming, especially for studies that are outdoors, the gain in accuracy was not what was expected (Hsien-Chou and Hong-Jhih 2009). Most standard deviations and mean pixel errors between manual and automatic calibration were within one pixel and verifies that manual calibration is still a viable, if not better, process of camera calibration (Hsien-Chou and Hong-Jhih 2009).

**2B. Mapping-Grade and Smartphone GPS Accuracy**

Accuracy in mapping-grade GPS devices and smartphones with GPS capability has improved over the past few years, but it is necessary to know the current state of accuracy and precision in these devices. Studies covering GPS accuracy consist of tests to measure error with mapping-grade GPS devices and smartphones with GPS capability (Firuzabadi and King 2012, Hodel 2013, Militino et al. 2013, Frank and Wing 2014). Militino points out that "uncertainty is also inherent in geospatial data" (Militino et al. 2013, p. 675). Factors outside of human control that can cause uncertainty and compromise the quality of GPS data include the atmosphere, the geographic location where a point was collected, and comparing time (Militino et al. 2013). No specific test can solve all accuracy issues that may occur when collecting GPS data (Firuzabadi and King 2012). Even if a study area is selected in order to avoid certain conditions that contribute to GPS location data uncertainty, tests reported in literature provide a better understanding of what to expect outdoors collecting GPS data.

Atmospheric disturbances interfere with signals sent from satellites to any GPS. The upper atmosphere slows down signals sent from the satellite, which "delays the signals arrival at the receiver, thereby affecting the distance calculation"(Militino et al. 2013, p. 675). GPS positional errors "are not completely independent of the locations"(Militino et al. 2013, p. 675). Geographic location, especially "valleys or mountain regions with high degrees of humidity"(Militino et al. 2013, p. 684) can contribute to location errors. Using mapping-grade receivers on rainy days may yield larger errors, averaging over 1m larger in root mean square error than points collected by the same method on a dry day (Frank and Wing 2014).

Time is another issue researched in recent studies with GPS accuracy. Clocks in satellites are almost perfect (Militino et al. 2013, cited Han et al. 2001, Kenneth Sr et al. 2008, Huang and Zhang 2012), but "clocks in receivers are not as good"(Militino et al. 2013, p. 676). Devices with GPS capabilities, like smartphones, used by researchers and consumers feature "an independent clock, not synchronized with GPS, and thus, the implementation of the GPS time-tagging may vary over a large range"(Seube et al. 2012, p. 85). To account for time errors in high-quality GPS devices, post-processing software packages like Pathfinder Office by Trimble® correct GPS position errors by referencing "continuously operating reference station (CORS) base stations, which apply corrections to data based on known locations and time-dependent coordinate estimates"(Frank and Wing 2014, p. 391). Even though time error can be resolved with certain software packages, "the estimation of the latency is mostly left to the end user"(Seube et al. 2012, p. 85). These types of GPS locations, corrected in real time or post-processed, were used for camera calibrations in this study. GPS devices capable of collecting locations and times with submeter accuracy and millimeter precision are helpful in generating reliable camera calibration models from GPS locations.

Smartphones, since their birth in 2006-2007, and the GPS chips featured in them have improved over the past 8-9 years, but their location accuracy, provided from a smartphone's GPS, is not well understood. Jonathan Hodel (2013) tested accuracy performance with an iPad 4 LTE, an iPhone 4S, and a Motorola Droid RAZR MAXX when benchmarked against a Trimble® Geo XH with real-time kinematic correction (2013). All registered coordinates from mobile devices fell within a twenty foot radius of the Trimble® device (Hodel 2013). Most of positions from the devices were between four and fifteen feet from the benchmark (Hodel 2013). While smartphones' GPS capabilities have improved and the locations given by them assist with

tasks like navigation, smartphones with GPS capabilities should not be relied on for activities requiring high accuracy and precision like surveying (Hodel 2013).

A more sophisticated test done by Paul Zandbergen (2011) looked at mobile phone accuracy when tested at known coordinates in three different scenarios: "static outdoor, static indoor and dynamic outdoor" (Zandbergen and Barbeau 2011, p. 387). For the static outdoor test, Zandbergen (2011) had the two mobile phones used for his testing, a Sanyo SCP-7050 and a Motorola i580, mounted on a survey tripod and collected locations from each phone at two second intervals over a 75-minute period. The two second intervals provided the "fastest rate that could be achieved across all units for reliable logging" (Zandbergen and Barbeau 2011, p. 387) The two mobile phones were also compared to two consumer-grade GPS devices: a Garmin 76MAP and a Trimble® Juno ST. Results from these tests (Zandbergen and Barbeau 2011, p. 389) show all of the positions collected from the Garmin and Trimble® devices to be within five meters of the intended location, while the mobile phones showed scattered location results. Some of the locations from the phones were within one meter of the benchmark, but some of the locations were as far as sixty meters away (Zandbergen and Barbeau 2011). What stood out from these studies is that while mobile phone GPS locations can be accurate at times, there is little to no consistency in getting repeated accuracy. The differences could be problematic if someone wants to use a smartphone's location to locate someone on an image.

One note to make in regards to the mobile phones used in these studies is the difference in how the location is collected in comparison to a mapping-grade GPS device. Mobile phones use what is called Assisted GPS, A-GPS for short. A-GPS assists the mobile phone in the initial process of collecting the location information from a series of satellites (Zandbergen 2009). As a means to reduce power consumption by the mobile phone and the time it takes for a phone to

retrieve an initial location, "many of the functions of a full GPS receiver are performed by a remote GPS location server" (Zandbergen 2009, p. 6). This remote GPS server provides information about the satellites used to derive the phone's location and sends that information over the cellular network (Zandbergen 2009). In areas where satellite visibility is limited, like urban areas, other means to derive locations are also employed to compensate for the lack of satellite visibility. These include "cellular network signals, Wi-Fi signals, Bluetooth, infrared, ultrasound or other radio frequencies" (Zandbergen 2009, p. 7). These alternative methods used in A-GPS are important to understand when comparing locations collected on different GPS devices.

**2C. Location-Based Social Network Data (LBSN)**

LBSN Data and research pertaining to it has become increasingly popular over the past few years. Social networking sites, like Twitter, have large amounts of geo-tagged social network data, which help analyze spatial trends and distribution from events. The main collection method of LBSN data is data mining, which is "the process of analyzing data from different perspectives and summarizing it into useful information" (Palace 1996). Databases like MongoDB assist users in mining through LBSN data in order to collect data from a specific location and set of keywords in that specific location. LBSN data is applicable (Staton 2013) and very relevant in this study due to the possibility of using locations from certain LBSN data to identify someone. Earthquake reporting, predicting presidential elections, and recommending travel locations are a few of the many ideas generated from collection of LBSN data (Sakaki et al. 2013, Majid et al. 2013, Tsou et al. 2013).

Twitter "has real-time characteristics that distinguish it from other social media such as blogs"(Sakaki et al. 2013, p. 930). Sakaki et al. (2013) researched tweets and their locations as a

means for “real-time event detection”(Sakaki et al. 2013, p. 919) to find out where an earthquake may have started. Twitter updates in real-time, so this LBSN data may be used to implement a system which notifies users inside a defined area of an imminent natural disaster, like an earthquake (Sakaki et al. 2013). Twitter users, if they allow it, can tag a location to a tweet. Such location data can localize the area from which someone is reporting (Sakaki et al. 2013).

Social movement mapping is another area that has become possible with the availability of LBSN data (Tsou et al. 2013). Tsou et al. (2013) use geolocated tweets connected to the 2012 United States Presidential election in an attempt to map shifts in popularity on Twitter between Barack Obama and Mitt Romney. To ensure tweets in the study were unique to a specific user, retweets and computer generated tweets were referred to as “”Noise”, “errors”, “biases”, and “distortion””(Tsou et al. 2013, p. 342). If all noise can be separated from the more unique tweets, “researchers might be able to reveal important social contexts of specific events…and understand the temporal and spatial relationships among these short messages and human behaviors” (Tsou et al. 2013, p. 347).

Posting about travel experiences and reviewing tourist destinations are also popular on social networking sites (Majid et al. 2013). Majid et al. (2013) use algorithms and models to personalize, based on social media habits and LBSN data, a user’s travel experience. This has facilitated a “need for a system that recommends tourist locations to match the tourists’ interests” (Majid et al. 2013, p. 663). Majid et al. (2013) focused on three areas to develop this system: Collective wisdom, personalization, and context awareness. Spatial location is connected to context awareness, because where a person may want to go will depend on where that person is at the moment, and weather conditions outside (Majid et al. 2013). Some tourist areas may be more preferable to visit on a rainy day, like a museum, instead of a park (Majid et al. 2013).

While LBSN data has been implemented in the aforementioned scenarios (Sakaki et al. 2013, Tsou et al. 2013, Majid et al. 2013), and researchers are continuing to add to this area at this point in time, the research described in previous literature has not necessitated a need for near submeter accuracy in LBSN data. Majid et al. (2013) point out that the location tagged on their LBSN data from Flickr provides only latitude and longitude. The lack of elevation data may prove problematic, but that is relative to the spatial resolution and surface being recorded if someone wants to locate a tweeter (Erdem and Sclaroff 2004).

Previous research on Twitter, its location data, and cameras at Virginia Tech has also paved a way for this study. In 2012, Peter Sforza and Kyle Schutt demonstrated the possibility of linking social network posts to webcams in their "I Can See You Tweet" presentation (Sforza and Schutt 2012). This project consisted of a tweeter standing in front of a webcam while tweeting and including the "#burrusswebcam" hashtag in their tweet. That hashtag would trigger the webcam to take a snapshot at that time and send the image to the tweeter's phone. A paper presentation by Sforza, Charles Staton, Kyle Schutt, and Thomas Dickerson at the 2013 UCGIS conference in Washington, DC expanded on Sforza and Schutt's 2012 project in regards to the overall progress in connecting data from social networks to "internet based video cameras"(Sforza et al. 2013). These projects and studies on LBSN data provide a clearer understanding of what is possible in this study and future research.

**2D. Next-Generation 911**

With the need to better serve constituents in the digital age, the FCC has recently updated its policies in regards to wireless location accuracy under Next-Generation 911 (Federal Communications Commission 2015). While not directly related to this study, the use of location in public safety is very relevant in regards to being aware of the progress of location accuracy for

use in emergency environments. In this policy update from January 2015, the FCC delineated a six-year and eight-year plan that hopes to have Commercial Mobile Radio Service Providers (CMRS) provide more accurate horizontal and vertical locations from wireless devices during emergencies. For horizontal accuracy, the CMRS provider must provide 40 percent of its wireless 911 calls with "[a] dispatchable location or [a] XY locations within 50 meters" (Federal Communications Commission 2015, p. 3) within two years. By 2021, all CMRS providers should be supplying at least 80 percent of their wireless 911 calls with this accurate location data (Federal Communications Commission 2015). For vertical accuracy, nationwide CMRS providers need to "develop a proposed z-axis accuracy metric" (Federal Communications Commission 2015, p. 3) that needs to be approved by the FCC within three years. In the vertical accuracy requirements, the FCC also requires those providers that have the technology designed to retrieve vertical location to deploy that within eight years to the top 50 cellular market areas (CMA) (Federal Communications Commission 2015). These location requirements set forth by the FCC earlier this year show the importance location can be when someone is calling 911. This implementation should also help with deriving locations in urban areas and in buildings with multiple floors. This technology would assist first responders with getting accurate location data and act quicker in emergency situations.

**2E. Conclusion**

Reviewing articles and research from similar backgrounds provided helpful insight for research reported in this study. There are areas, however, where methodology and intent differed. These differences did not negate the need to apply suggestions from literature and research to improve this research and areas to improve future research. While error was expected in this study, the amount of error measured from GPS locations collected on a Trimble® GeoXT

2005 Series and an iPhone 5s should still allow someone to be located on an image based upon their GPS location. The results and future suggestions provided from previous research offered a more fine-tuned approach to the methodology and how to address shortcomings from previous studies.

## 3. Methods, Data Retrieval, and Analysis

While Staton's (2013) work on surveillance cameras and location based social network data only studied the accuracy of tweet locations on an image, the goal in this experiment was to see if mapping-grade GPS points can be tied to a surveillance camera image to calibrate the image to the earth coordinates it views and, if so, possibly to identify a person at that collected the GPS location. A second test with GPS points collected from an Apple iPhone 5s was performed on the same calibration models to see if the location collected from an iPhone GPS affected the predicted locations given by the calibration models. I hypothesize that, after running differentially corrected and smartphone GPS points through multiple-regression models generated from manual camera calibration, I should be able to locate myself on a surveillance camera based on the time and location a GPS point was collected. In order to generate a reliable system, the differentially corrected GPS points and smartphone GPS points need be located within one meter of the intended location. **Figure 1** shows a diagram of what this system, in relation to the area of study, would do. Four GPS satellites in orbit while the person in the camera viewshed tweets from his/her phone provide a location based on those four satellites and a nearby cell tower. The GPS XYZ location is then mapped to pixel coordinates on the image from the camera after running each location attribute (XYZ) through its respective regression model.

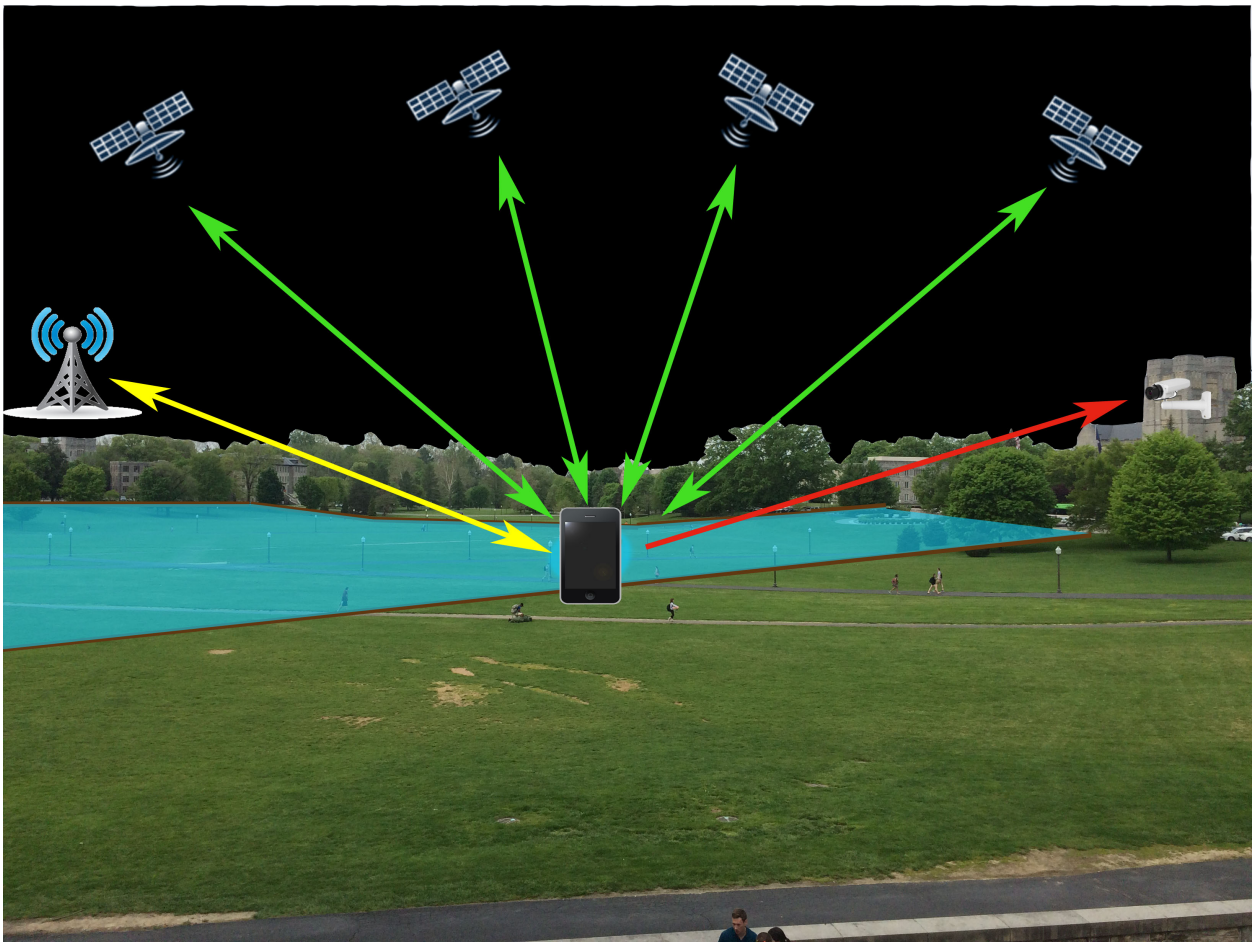

**Figure 1 - Sketch of processing GPS locations and projecting them in a camera image. The phone relies on GPS satellites (satellites with green arrows) and nearby cell towers (tower with yellow arrow) to assist in collecting a location. The location is then projected onto the camera image (red arrow) overlooking the viewshed (light blue).**

The mapping-grade GPS device used for the camera calibration is a Trimble® GeoXT™ 2005 series GPS that has the ability to retrieve locations with submeter accuracy and millimeter precision. The 115 GPS reference points collected for the calibration were in Universal Transverse Mercator (UTM) coordinates. To avoid issues with vertical error, the Trimble® GPS was placed on the ground during point sampling. The first series of reference points used to calibrate the surveillance camera were easily identifiable in the image, like a corner of a walkway or the foot of a light post. Most of these identifiable points were concentrated near the middle of the image, so more reference points throughout the entire view needed to be collected. Points that were not identifiable on the ground were marked on a screenshot of the camera's

viewshed in as even distribution as possible. The marked up image showing all of the points to collect was used as a reference map throughout the collection process. After the collection of reference points, the Trimble® GPS reference points were differentially corrected. Trimble's Pathfinder software was used to differentially correct each point by retrieving location data from the nearest Continuous Operating Reference Station (CORS) in Blacksburg, VA (Kaplan and Hegarty 2005, p. 379).Finally, the corrected points were matched manually to their respective two-dimensional pixel locations on the image (**Figure 2**).


**Figure 2 - Locations on Image where Calibration Points were collected.**

The entire collection process recorded by the network camera was downloaded onto a computer in order to capture screenshots and locate each collection point's pixel coordinates. The Axis P1354 network camera used in this study serves as a public webcam overlooking the

Drill Field at the Virginia Tech campus. This camera records square pixel video at a resolution of 1280 by 960 at about 28 frames per second. Photo editing software like GIMP allows one to navigate an image reporting pixel coordinates at the mouse pointer. The pixel coordinates from each location the GPS was placed on the ground were entered into an Excel table that included each pixel coordinate's differentially corrected Trimble® GPS reference point XYZ location. This table was used to generate two calibration models in JMP: one formula to convert Trimble® GPS reference points (X, Y, and Z) to a pixel on the X-Axis and a second to convert the Trimble® GPS reference points to a pixel on the Y-Axis (**See Appendices A-E**). Lens distortion was easy to detect on the images collected from the camera, which lead to the use of curvilinear multiple regression models to account for this distortion and the uneven surface of the study area.

After the curvilinear calibration models were generated, adjusted $R^2$ values were calculated, but residuals at each point were mapped onto the image in order to get a better idea of what accuracy the models achieved and to identify any spatial patterning of errors. Displaying errors in a visual manner is very helpful and "can be interesting for users and GPS professionals" (Militino et al. 2013, p. 675). Each reference point and the predicted point were mapped on the entire image. Applying the Pythagorean theorem derived a straight-line distance between the two points. These straight-line distance residuals were used to map the distance in the image between the actual and predicted locations from the models. Residuals generated from these models determined that use of a single model for the entire image generated larger residuals as one moves from the center of the image, and that zone-based curvilinear regression models were necessary.

The use of zone-based calibration models was based upon the realization that residuals were too large to provide many areas on the image where someone could likely be located. In

order to generate more fine-tuned calibration models, four zones were outlined on the image (**Figure 3**). These zones were selected by outlining areas in the image that had visible amounts of lens distortion, low spatial resolution, and high spatial resolution. The area of the image where someone could be located (or possibly even identified) based on attire and physical attributes is in the lower center of the image, or the "Lower Zone". The other zones outlined in the image were the Left, Upper, and Right Zones. The left and right zones cover the sides of the image where lens distortion is most apparent. The upper zone in the image covers part of the Drill Field and has a fairly low spatial resolution throughout the zone. Although the Lower Zone has the highest spatial resolution in the image, it is not as high as desired to implement in a real-world environment if one wanted to identify and not just locate a person. The camera in use would need to be placed closer to the area of interest or zoom in to the location of interest in order to take advantage of more spatial resolution in the entire image (Erdem and Sclaroff 2004). The Trimble® GPS XYZ reference points in each zone were selected, and two curvilinear regression models converting those points to Pixel X and Pixel Y (**See Appendices A-E**) generated for each zone, and the residuals from each pair of models were analyzed and mapped in the image. The residuals at this time were in pixels, so, to convert to an approximate ground distance, an average pixel width in each zone was calculated.

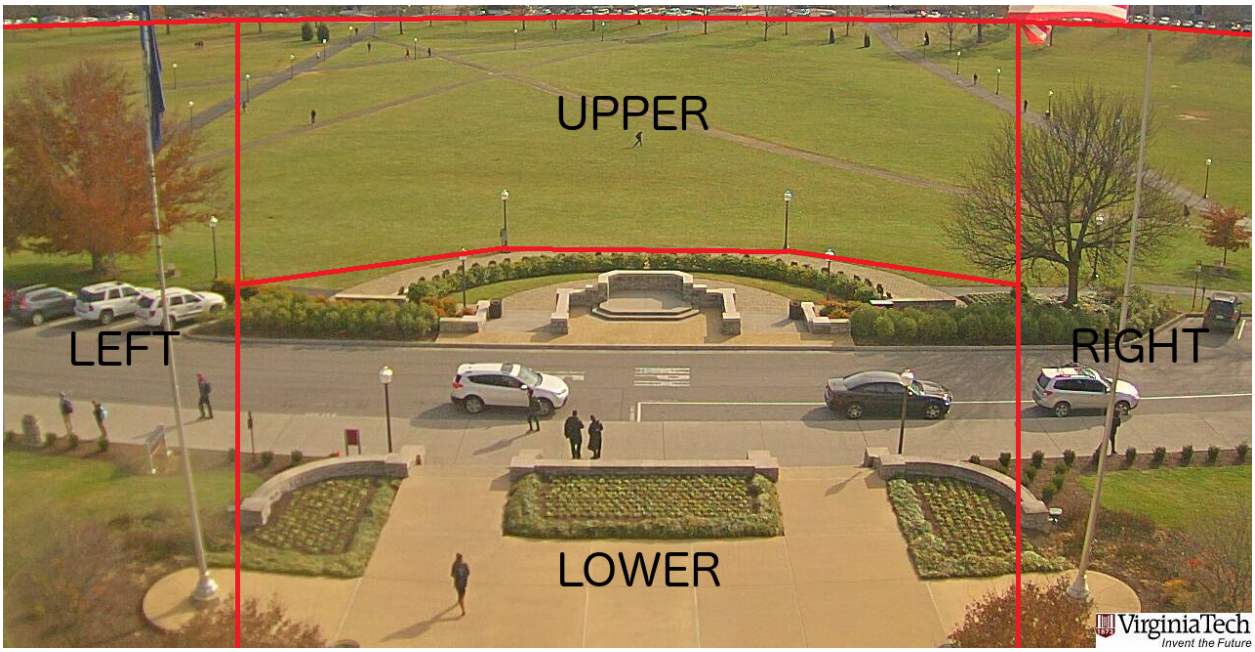


**Figure 3 – Four zones depicted on the area used in the study.**

After completing the Trimble® GPS reference point collection and calibration model generation, iPhone 5s GPS points were collected at locations where reference points had been collected to see how a smartphone's GPS location would perform using the calibration formulas generated from the reference points. The Trimble® Navigator App for iOS was used to collect the XYZ location at each point in UTM coordinates.

## 4. Results

Only 108 of the 115 reference points collected in the study area could be used in the regression models. The vetting process for the reference points took place while reviewing the downloaded camera feed which recorded the entire collection process. Multiple issues contributed to removing seven reference points from the area study. One reference point did not have location data because of a loss of GPS signal during the point collection. Several reference points were removed from the analysis because they were erroneously collected outside the view shed. Glitches also occurred in the playback of the camera stream, causing the video to skip a couple of seconds ahead at multiple instances, including the image of one reference point, which was therefore removed from the study.

The two curvilinear regression models using cubic functions produced adjusted $R^2$ values of 96.82 percent for the predicted Pixel X locations and 96.77 percent for the predicted Pixel Y locations across the entire image. Adjusted $R^2$ values that high were impressive, but placing the residuals derived from the models back on the image showed that the models were not as accurate as desired (**Figure 4 and Table 1**). The least amount of error is around the central area of the image and the residuals increase as the distance from the center increases. The lens distortion, uneven surface of the study area, larger area to account for in this calibration may have contributed to the error that could not be accounted for by these two models.

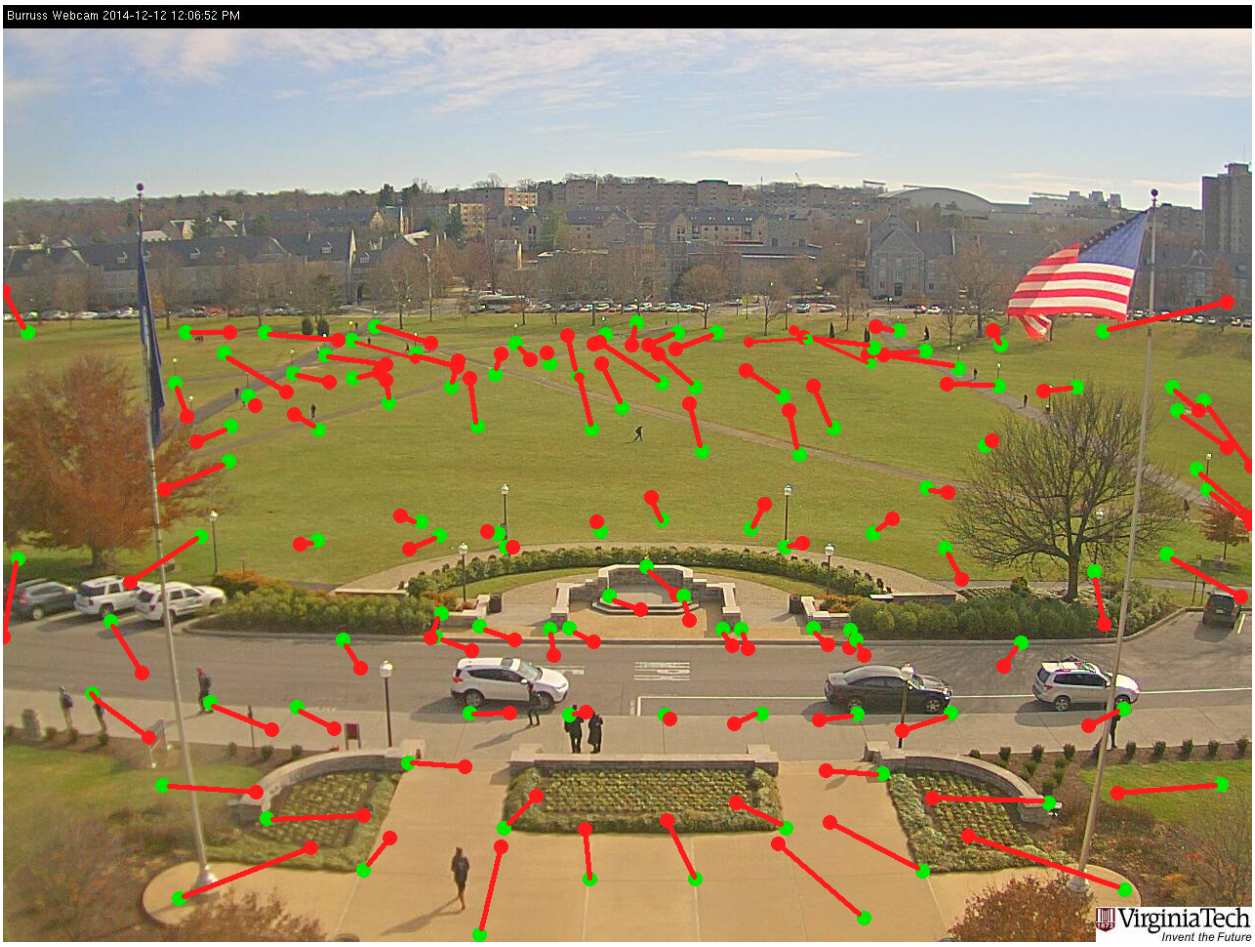


**Figure 4 – Residuals produced from the Curvilinear Multiple Regression Model calibrated to the entire image. Reference Points (Green) compared to the Predicted Point (Red).**

| | **Adjusted $R^2$ for X (Percent)** | **Adjusted $R^2$ for Y (Percent)** | **Mean Residual (Pixels)** |
|---|---|---|---|
| Entire Image | 96.82 | 96.77 | 51.6 |

**Table 1 - Adjusted $R^2$ Values and residuals from the model calibrated to the entire image.**

The same calibration model parameters used for the calibration of the entire image were also used in each of the four zones, giving a total of eight models from this adjustment. Once the residuals were derived and mapped, the results from using a zone-based approach were better than calibrating the dataset to the entire image (**Table 2**).

| Zone | Adjusted $R^2$ for X (Percent) | Adjusted $R^2$ for Y (Percent) | Mean Residual (Pixels) |
|---|---|---|---|
| Left | 91.07 | 99.32 | 11.5 |
| Upper | 99.83 | 99.66 | 8.0 |
| Right | 98.91 | 99.39 | 6.5 |
| Lower | 99.75 | 98.02 | 12.7 |

**Table 2 – Residuals (in pixels) from splitting the models to cater to each zone.**

The adjusted $R^2$ for the zone-based models reached as high as 99.75%. Mean residuals (in pixels) in the three areas outside the lower zone were actually lower than the mean residuals in the lower zone. However, some zones were closer to the camera than others, meaning that pixels vary in coverage depending on distance from the camera, and angle of view. Therefore, a scale was generated for each zone to convert pixels to meters. To estimate scales for each zone, three separate horizontal distances inside each zone from pairs of GPS reference points having nearly the same Pixel Y coordinate (a value within 1-2 pixels) were calculated to estimate a ground distance based on pixel width. This step required dividing the three-dimensional distances between two Trimble® GPS reference points by the number of pixels in the image between the reference points. After calculating the pixel width, the three widths from each zone were averaged in order to generate an average scale for each zone. Using these scales was helpful to convert the distance from where a reference point was collected to where it was placed on the image by the calibration models (**Table 3**). If it is feasible to identify a person in an image, such as clothing, mean errors at or below one meter from the intended location would reduce the time and effort to locate someone on an image. These low errors produce a smaller search radius, which in turn would make it more likely that the correct person is located on the image.

| Zone | Average Pixel Width (m) | Mean Error (m) |
|---|---|---|
| Left | 0.1481 | 1.7032 |
| Upper | 0.1283 | 1.0264 |
| Right | 0.1282 | 0.8333 |
| Lower | 0.0425 | 0.5398 |

**Table 3 – Average width of pixel in all four zones along with the residuals in pixels converted to distance in meters.**

A confidence band was derived in each zone to assist the use of the scales. These bands provided an area where a mapping-grade GPS point should land with 95% certainty. The bands for each zone were determined from the mean distance between each reference point's upper and lower 95% confidence intervals for the predicted Pixel X and Y locations. Mean distances calculated from these were used as the diameter for the confidence band. The confidence bands also helped determine the level of certainty one should have if they want predicted points to be placed within a certain distance of the location a point was collected (**Figure 5 and Table 4**).

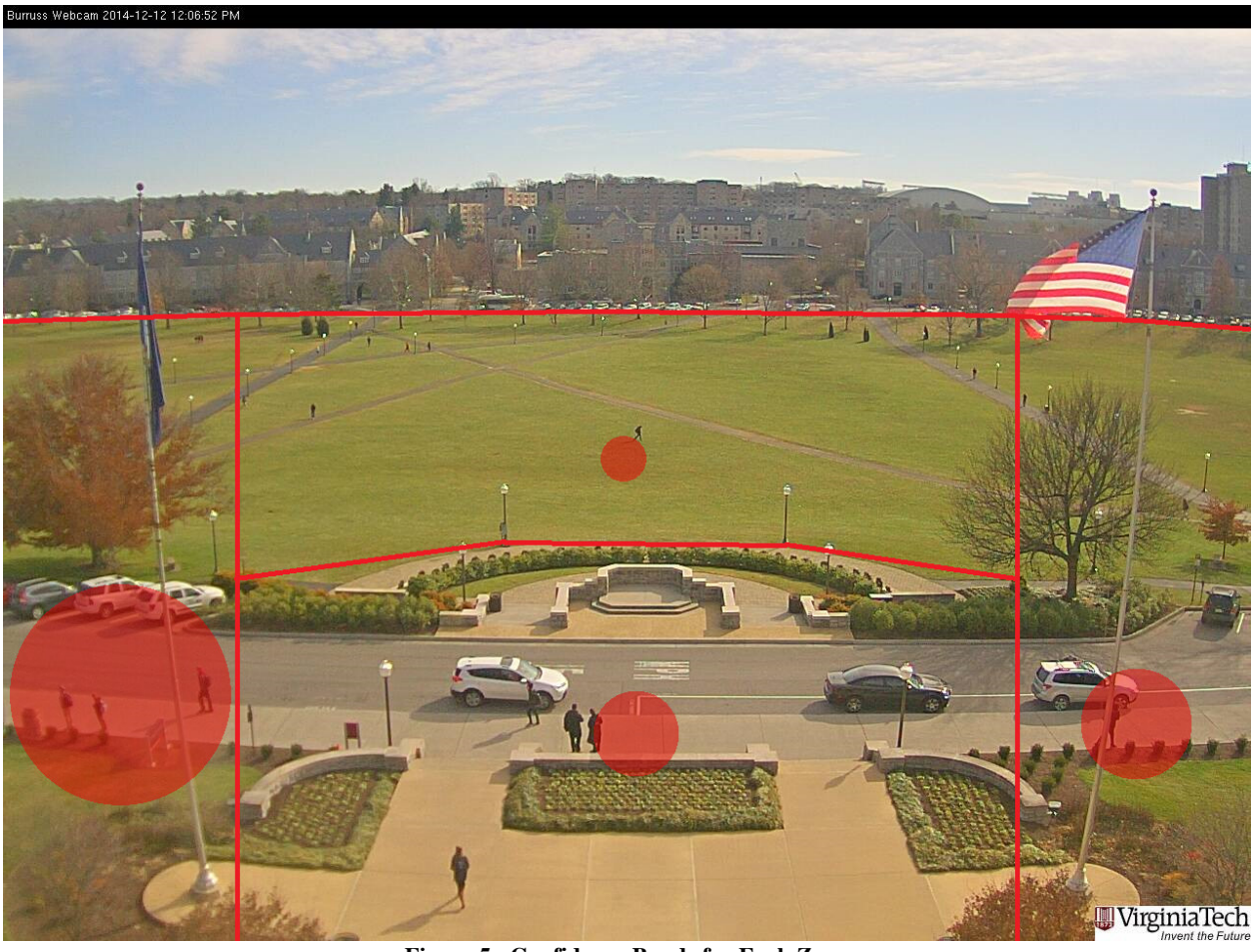


**Figure 5 - Confidence Bands for Each Zone**

| Zone | Radius of 95% Confidence Band (pixels) | Radius of 95% Confidence Band (m) |
|---|---|---|
| Left | 115.2 | 17.061 |
| Upper | 23.4 | 3.002 |
| Right | 57.7 | 7.397 |
| Lower | 44.4 | 1.887 |

**Table 4 - Confidence Band Radius in Pixels and Converted to Meters via Pixel Widths from Table 3**

While the predicted reference points were placed very close to their respective locations on the ground, the GPS time associated with each point was difficult to measure with precision. While the camera's time and the GPS time looked to be within a second of each other, no visual signal was provided in the video feed to note the exact time a location was collected. Reference points used for the camera calibration were precise to the second, but it was difficult to find the exact frame in the video without a visual signal. Therefore, it was estimated that the GPS time and camera time were within 1-2 seconds of each other. If a person is walking at a normal pace in front of the image, which would be around 3 mph, a time lag of 1-2 seconds (30-60 frames) between the GPS and the camera could inaccurately place the GPS location on the image.

To test these zone-models in a "real-world" scenario, one in which people do not carry around $5000 GPS units and lay them on the ground to measure their locations, an iPhone 5s with Location Services activated was used to collect points at all locations at which Trimble® GPS reference points had already been collected. The first phase of iPhone point collection was to collect points at locations easiest to detect on an image: edges of sidewalks, bases of light poles, or corners of columns. In order to collect a similar number of iPhone points in each zone, a second phase of collection occurred. Using a sample of the reference points, the Trimble® GPS unit was used to navigate to the open areas on the image where a previous reference point was located, and an iPhone point was then collected. As it is more realistic to a tweet or posting from a phone GPS, the iPhone points were collected at waist level, which measured around one meter high, instead of on the ground. Because the Trimble® Navigator application displays elevation to

within a meter, one meter was subtracted from each elevation value to reflect the change from waist level to ground level.

The iPhone point coordinates were then compared to their respective reference points in order to analyze location errors between the two locations. The reference points were located with submeter accuracy and millimeter precision. The iPhone points' were not as accurate, as the locations collected varied between 0.9 and 10.93 meters from the reference point (**Table 5**). Once the iPhone points were analyzed, they were entered into their respective regression equation by zone. Residuals from each model showed that the iPhone's reduced accuracy contributed to higher residuals after being run through the models (**Figure 6**).

| Zone | Minimum Distance from Reference point (m) | Maximum Distance from Reference point (m) | Mean Distance from Reference point (m) |
|---|---|---|---|
| Left | 2.72 | 6.93 | 5.09 |
| Upper | 2.27 | 10.93 | 5.22 |
| Right | 0.90 | 8.07 | 3.82 |
| Lower | 1.10 | 10.51 | 4.17 |

**Table 5 – Phone errors in distance (meters) from the respective Trimble® GPS reference point.**

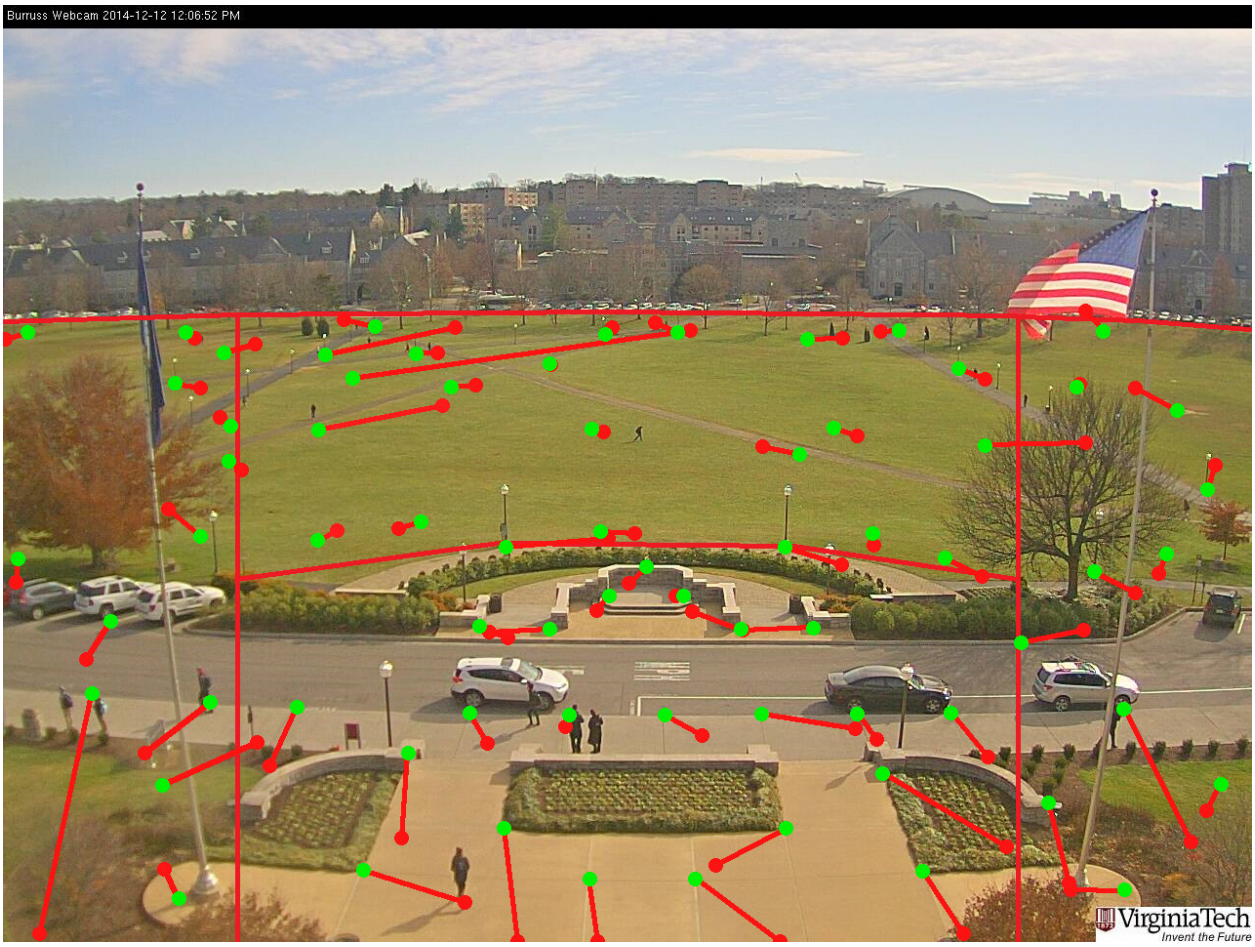


**Figure 6 - Phone Residuals Resulting from Zone-Based Calibration Models. The places on the ground where each iPhone location was collected (green) compared to where the zone-based regression equations placed the iPhone locations on the image (red)**

In order to estimate the ground distance between each modeled iPhone point and the location on the image where the iPhone points were collected, the scale system used previously (**Table 3**) was applied. From these scales, an average distance error was calculated for each zone in meters. The mean straight line residual (in pixels) from each zone was multiplied by the average pixel width in each zone to get the straight-line residual distance converted from pixels to meters. The results show that the mean distance from the collection point (**Table 6**) is not similar to the mean straight-line distance from the iPhone location to the reference point location (**Table 5**).

| Zone | Mean Residual from Collection Point (Pixels) | Mean Residual from Collection Point (m) |
|---|---|---|
| Left | 55.0 | 8.15 |
| Upper | 53.9 | 6.92 |
| Right | 51.4 | 6.59 |
| Lower | 67.8 | 2.88 |

**Table 6 – Mean Distance Residuals of iPhone points from their respective collection points in the image. Measured in Pixels and converted to meters**

To compare the iPhone points to reference points in the lower zone, three locations were marked on a subset of images inside the lower zone: For each sample, the point on the image where the reference point was collected; where the reference point was predicted; and where the iPhone location was predicted. In the lower zone, the average distance between the location each point was collected at on the image and where the models predicted each location was about 2.88 meters. **Figure 7** shows that result and the high accuracy of the reference point compared to the low accuracy of the iPhone 5s point.

**Figure 7 – Example of points collected in surveillance zone. Green = Collection Point; Red = Predicted Trimble® GPS reference Point; Blue = Predicted iPhone Point.**

The example in **Figure 7** shows the predicted Trimble® GPS reference point was placed much closer, 23 pixels to be exact, to its collection location in the image. After conversion from the lower zone average pixel width (**Table 3**), the point fell about 0.978 meters away from the actual location on the image where the reference point was collected. The iPhone 5s point collected at the same location was placed 109 pixels, or about 4.632 meters away. These points could still be used to possibly locate a person on an image, but it would be relative to that person's surroundings and the density of persons in front of a camera.

Let's assume that the person to be located must be the closest to the pixel point identified by the calibration model. Clearly, the more dense the population in the area, the less room for error in the GPS location from the smart phone. In order to simulate variable pedestrian density to determine whether or not a phone's GPS location could be used to locate a person on an image, three pedestrian density levels inside each zone were generated. This test provided an opportunity to determine at what pedestrian density locations from a phone or GPS may no longer be reliable when trying to use that location to locate a person on an image. Three density levels were used in this test: Low (10 random pedestrian points), Medium (25 random pedestrian points), and High density (50 random pedestrian points). The Medium-density level pedestrian points from the lower zone are shown in **Figure 8** alongside a phone collection point. The expected nearest neighbor equation was run inside each zone at each density level to determine the expected nearest neighbor distance, assuming a random pedestrian distribution. These distances, given in pixels, were subsequently converted to meters using the same conversions described above for each zone.

**Figure 8 – Pedestrian Density Test Example. The iPhone collection point (Green) along with the predicted location (Blue) compared to the 25 Medium-density pedestrian points (Red) randomly generated inside the lower zone. The expected nearest neighbor distance is outlined by the yellow circle.**

After comparing the converted residuals to the distances from neighboring pedestrian points, all of the Trimble® GPS reference point residuals were smaller than the distance to each reference point's nearest neighbor throughout all of the densities under the assumption of random placement. This ensures that the Trimble® GPS reference points would correctly link back to the collection point when the closest point was selected. While 100 percent of the Trimble® GPS reference points would match properly to their respective collection points, the same cannot be said for the iPhone's points. Since the spatial resolution is not the same throughout the entire image, **Tables 7, 8, and 9** provide the nearest neighbor distances in meters for the three pedestrian density levels inside each zone. These tables (**Tables 7, 8, and 9**) show the distances (in meters) that separate random nearest neighbors in each area of the zone. Three different pixel widths were calculated in each zone to get distances that would better reflect the nearest neighbor distance based on where in the zone a pedestrian is located. Results from this

testing shows that, as density increases, the chance of linking an iPhone GPS point back to its sender's location decreases (**Table 10**).

| Zone | Low Density | Medium Density | High Density |
|---|---|---|---|
| Left | 2.78 | 1.76 | 1.24 |
| Upper | 5.53 | 3.50 | 2.47 |
| Right | 2.76 | 1.74 | 1.23 |
| Lower | 2.81 | 1.78 | 1.26 |

**Table 7 – Nearest neighbor distances (in meters) for the lower area inside each of the four zones**

| Zone | Low Density | Medium Density | High Density |
|---|---|---|---|
| Left | 5.11 | 3.23 | 2.29 |
| Upper | 10.23 | 6.47 | 4.58 |
| Right | 9.81 | 6.20 | 4.39 |
| Lower | 4.13 | 2.61 | 1.85 |

**Table 8 – Nearest neighbor distances (in meters) for the middle area inside each of the four zones**

| Zone | Low Density | Medium Density | High Density |
|---|---|---|---|
| Left | 15.57 | 9.85 | 6.96 |
| Upper | 13.64 | 8.63 | 6.10 |
| Right | 11.14 | 7.05 | 4.98 |
| Lower | 5.27 | 3.33 | 2.36 |

**Table 9 – Nearest neighbor distances (in meters) for the upper area inside each of the four zones**

| Zone | Low Density | Medium Density | High Density |
|---|---|---|---|
| Left | 76.92 | 61.54 | 46.15 |
| Upper | 80.95 | 76.19 | 57.14 |
| Right | 72.73 | 45.45 | 27.27 |
| Lower | 70.83 | 37.50 | 29.17 |

**Table 10 – Percent of iPhone 5s points in which the residual is lower than the nearest neighbor distance**

There is a 70-80% chance in a low-density area that a phone's location could be linked back to the proper person and that percentage decreases with higher pedestrian densities. In more densely populated areas, using a phone's location data would be problematic because of the shorter distances between people. Though unrealistic at this time, points from a differentially corrected GPS would be optimal in medium to high-density urban environments.

## 5. Discussions and Conclusion

Calibrating differentially corrected GPS points to the entire image with curvilinear multiple regression models did not give the accuracy desired. The results improved after splitting the image into four zones, which allowed portions of the image to be calibrated based on a selected area of interest. From the zone-based models, predicted locations from the reference points were close enough to locate a person on an image in relation to the location on the image where the point was collected. Differentially corrected GPS points, when run through zone-based camera calibration models, can locate a person collecting a certain point on this image up to a density level of at least 50 pedestrians. The same thing cannot be said about the location collected from a smartphone. The ability to locate someone in an image based on the location collected from a smartphone would be relative to the pedestrian density of the area being covered. The zone-based models, even when calibrated to adjusted $R^2$ values nearing 100%, could not overcome the lack of accuracy and precision from the phone GPS points. Because of this, a smartphone's GPS location or any location-based social network data may not be accurate enough in medium to high-density areas to use as a means of locating someone on an image. The accuracy and precision of the location is the issue at hand with these results and not the model(s) used. This does not mean that locations from smartphones cannot be used for other reasons, as confirmed in prior literature.

To ensure issues out of one's control are minimized, it would be beneficial to use a camera under direct control by the researcher or group. The camera used, while helpful in this research, provided some issues during testing. Upon personal examination of the camera placement, the Axis P1354 used in the study is indoors and a window is between the camera and

outside area being recorded. The manual camera calibration, however, covered the issue with the window in this study since it was a calibration from ground coordinates to image coordinates. If a calibration method requiring the use of lens optics was used, additional image distortion from the window may have caused issues in the results. When future research relating to this is conducted, this issue should be addressed in models that use lens optics as parameters. The placement of the camera indoors also caused issues in testing. The length of the camera body is longer than the depth of the windowsill, which caused the camera's position to move any time the blinds were adjusted. As Hsien-Chou and Hong-Jhih (2009) previously mentioned in their study, these adjustments would require a new calibration. Collecting phone points at previous locations, which had a known differentially corrected location tagged to them from the Trimble® GPS data collected circumvented this issue in this research, but a manual calibration is clearly a poor solution if a camera is likely to move, pan or zoom on a regular basis.

Using one's own camera would also assist in the retrieval of the camera's intrinsic parameters, for example the effective focal length and distortion coefficient. These parameters would assist in measuring distance and locating persons on an image with more precision and possibly accuracy. These parameters should be available in many cameras' metadata. Having an effective focal length during the period of study would help users to determine sizes of objects inside an image. The less precise approach used in this study, averaging pixel width based on ground distance and pixel distance between two known points, is not as viable a method to use if precise measurements are required. It would be interesting however to see how models based on the lens optics of this camera compare to the statistical accuracy of this research.

One piece of equipment not available during this study which would assist in navigating back to previous reference points, if necessary, is a RTK (Real-Time Kinematic) antenna

attached to the professional-grade GPS similar to the one used by Hodel in his benchmark testing (2013). This would ensure greater accuracy and precision in the placement of reference points if someone needs to return to a certain place in a study area with no visible marker.

In line with Hsien-Chou (2009), one could see if a manual or automatic camera calibration method would make a difference in minimizing residuals in one's study area. Staton's (2013) research in the same study area did not account for the correct type of lens distortion, which contributed to his high residuals in tweet locations. It is possible to derive an algorithm that accounts for barrel distortion or find a way to correct the image with a counter-distortion before being processed through a calibration model.

A myriad of smartphones with GPS chips are available to consumers, so it is helpful to test multiple smartphones and location accuracy in the same study area (Hodel 2013). With the release of the iPhone 6 during this research, it would be helpful to see if the addition of a barometer makes the location from an iPhone 6 or 6 Plus more accurate (Apple 2014). Hodel's (2013) research on smartphone accuracy showed that, like the iPhone 5s used for this study, some of the locations given by the smartphones were within a meter of the benchmark GPS location, but the consistency in accuracy was not achieved.

Time latency is an issue that needs to be addressed further, especially if one were to use these methods on location-based social network data. The timestamp used by Virginia Tech that is placed on the stream from the Axis P1354 is retrieved from the National Institute of Standards and Technology, same as for anything connected to networks on Virginia Tech's campus. While not used in this study, tweet times collected through Twitter's Streaming APIs are precise to the second (2015). This would require a future study, similar to and expanding on Staton's (2013) research, to see if the second Twitter says a tweet was sent matches with the time on the image

that tweet was sent. The times connected to the Trimble® GPS points, which is the time the GPS locked onto satellites to get locations, precise to the second, but after comparing the GPS times to the times on the camera both times were within a second or two of each other. Using a marker or sign to show to the camera when a location was collected would make the time comparison more accurate and easier to measure.

Even though locations collected by iPhone 5s were not accurate enough to locate an individual person on an image except in low-density settings, locations collected from this study were accurate and precise enough for uses that would be helpful in public safety. If GPS sensors in future smartphones can collect locations with consistently high accuracy and higher precision, then it may be possible to identify someone in more areas covered by a camera based on a tweet or social network post made from a smartphone. This, however, would still depend on the pedestrian density in the camera view, the camera itself, and objects blocking the camera from capturing the entire surface. This capability is based upon access to imagery collected by individuals or institutions that may or may not wish to make it available for analysis. While that may bother some because of the possible invasion of privacy, the possibilities branching from this research could assist public safety departments in using location-based social network data to better serve their constituents.

## References


911, F. M., 2014. *FCC Data: 9 out of 10 Wireless 9-1-1 Calls in D.C. Lack Accurate Caller Location Information* [online]. Available from: http://findme911.org/news/fcc-data-9-out-of-10-wireless-9-1-1-calls-in-d-c-lack-accurate-caller-location-information/ [Accessed March 31 2015].

AGSI, 2015. *Social Media for Law Enforcement* [online]. http://www.go360.info: AGSI. Available from: http://www.go360.info/industries/social-media-for-law-enforcement [Accessed April 15 2015].

Apple, 2014. *iPhone 6 - Technology* [online]. Available from: https://www.apple.com/iphone-6/technology/ [Accessed April 1 2015].

Cable, M., 2005. *Calibration: A Technician's Guide*. Research Triangle Park, NC: ISA - Instrumentation, Systems, and Automation Society.

Cetin, A. E., *et al*. 2013. Video fire detection - Review. *Digital Signal Processing,* 23(6), 1827-1843.

Commission, F. C., 2014. *911 Wireless Services* [online]. Available from: http://www.fcc.gov/guides/wireless-911-services [Accessed March 31 2015].

Wireless E911 Location Accuracy Requirements 2015.

Communications, A., 2014. *AXIS P1354 Network Camera* [online]. Available from: http://classic.www.axis.com/en/products/cam_p1354/index.htm [Accessed December 7 2014].

Erdem, U. M. and Sclaroff, S., Optimal Placement of Cameras in Floorplans to Satisfy Task Requirements and Cost Constraints. ed. *OMNIVIS Workshop*, 2004.

Firuzabadi, D. and King, R. W. 2012. GPS precision as a function of session duration and reference frame using multi-point software. *Gps Solutions,* 16(2), 191-196.

Frank, J. and Wing, M. G. 2014. Balancing horizontal accuracy and data collection efficiency with mapping-grade GPS receivers. *Forestry,* 87(3), 389-397.

Han, S. C., Kwon, J. H. and Jekeli, C. 2001. Accurate absolute GPS positioning through satellite clock error estimation. *Journal of Geodesy,* 75(1), 33-43.

Hodel, J., 2013. *So What's My Accuracy??? Mobile Device GPS with iPad, iPhone & Android* [online]. Available from: http://cloudpointgeo.com/blog/2013/4/26/so-whats-my-accuracy-mobile-device-gps-with-ipad-iphone-android [Accessed December 2 2013].

Hsien-Chou, L. and Hong-Jhih, W., An Automatic Camera Calibration Method Using GPS-enabled Mobile Device. ed. *Advanced Communication Technology, 2009. ICACT 2009. 11th International Conference on*, 15-18 Feb. 2009, 760-763.

Huang, G. and Zhang, Q. 2012. Real-time estimation of satellite clock offset using adaptively robust Kalman filter with classified adaptive factors. *Gps Solutions,* 16(4), 531-539.

Kaplan, E. and Hegarty, C., 2005. *Understanding GPS: Principles and Applications*. Artech House.

Kenneth Sr, L., Ray and Beard, R. L. 2008. Characterization of periodic variations in the GPS satellite clocks. *Gps Solutions,* 12, 211-225.

Learned-Miller, E., 2011. *Introduction to Computer Vision* [online]. Available from: http://people.cs.umass.edu/~elm/Teaching/Docs/IntroCV_1_19_11.pdf [Accessed November 19 2013].

Majid, A., *et al*. 2013. A context-aware personalized travel recommendation system based on geotagged social media data mining. *International Journal of Geographical Information Science,* 27(4), 662-684.

Militino, A. F., *et al*. 2013. Mapping GPS positional errors using spatial linear mixed models. *Journal of Geodesy,* 87(7), 675-685.

Palace, B., 1996. *Data Mining - What is Data Mining?* [online]. Available from: http://www.anderson.ucla.edu/faculty/jason.frand/teacher/technologies/palace/datamining.htm [Accessed December 7 2013].

Sakaki, T., Okazaki, M. and Matsuo, Y. 2013. Tweet Analysis for Real-Time Event Detection and Earthquake Reporting System Development. *IEEE Transactions on Knowledge and Data Engineering,* 25(4), 919-931.

Seube, N., Picard, A. and Rondeau, M. 2012. A simple method to recover the latency time of tactical grade IMU systems. *ISPRS Journal of Photogrammetry and Remote Sensing,* 74, 85-89.

Sforza, P. and Polys, N., 2010. Situational Awareness via Video Analytics incorporating video metadata into 3D models. VT Center for Community Security and Resilience Planning: Virginia Tech CGIT and IBM Exploratory Video Analytics Research Group.

Sforza, P. and Schutt, K., "I Can See You Tweet" Demonstration of the Fusion of Webcams and Location Based Services ed. *Virginia Association for Mapping and Land Information Systems (VAMLIS)* September 10 2012 Charlottesville, VA.

Sforza, P., *et al*., 2013. Linking Location Based Social Networks and Internet based Video Cameras. *Collaboration Across Communities: GIScience 2.0 and Beyond*. Fairfax, VA.

Staton, C., 2013. *Citizens as Sensors: Examining Tsai's Camera Algorithm Using a Location Based Social Network and Smartphone GPS Capabilities*. Project (Master's of Science). Virginia Polytechnic Institute and State University.

Tilden, D., *et al*., 2011. Multimedia mashups for mirror worlds. *Proceedings of the 16th International Conference on 3D Web Technology*. Paris, France: ACM, 155-164.

Tsai, R. Y. 1987. A Versatile Camera Calibration Technique for High-Accuracy 3D Machine Vision Metrology Using Off-the-Shelf TV Cameras and Lenses. *Robotics and Automation, IEEE Journal of,* 3(4), 323-344.

Tsou, M. H., *et al*. 2013. Mapping social activities and concepts with social media (Twitter) and web search engines (Yahoo and Bing): a case study in 2012 US Presidential Election. *Cartography and Geographic Information Science,* 40(4), 337-348.

Twitter, 2015. *The Streaming APIs* [online]. Available from: https://dev.twitter.com/streaming/overview [Accessed April 1 2015].

Zandbergen, P. A. 2009. Accuracy of iPhone locations: A comparison of assisted GPS, WiFi and cellular positioning. *Transactions in GIS,* 13(s1), 5-25.

Zandbergen, P. A. and Barbeau, S. J. 2011. Positional Accuracy of Assisted GPS Data from High-Sensitivity GPS-enabled Mobile Phones. *Journal of Navigation,* 64(03), 381-399.

# Appendix A
## Regression Formula used to calibrate Trimble® GPS XYZ to Pixel X in the entire image

37373445.0417186 + 15.1736647900555 * Z + (Z - 623.531722222222)
* (Z - 623.531722222222) * 0.577298202950854 + (Z - 623.531722222222)
* (Z - 623.531722222222) * (Z - 623.531722222222) * -0.569453603188171

+ -7.95150998077722 * Y + (Y - 4120320.76712037) * (Y - 4120320.76712037)
* -0.0689560538827739 + (Y - 4120320.76712037) * (Y - 4120320.76712037)
* (Y - 4120320.76712037) * -0.000308500376238664

+ -8.38029873658969 * X + (X - 551230.813768519) * (X - 551230.813768519)
* 0.0647011683676686 + (X - 551230.813768519) * (X - 551230.813768519)
* (X - 551230.813768519) * -0.000224685383877132

## Regression Formula used to calibrate Trimble® GPS XYZ to Pixel Y in the Entire Image

(-8503378.28731865) + -14.458289242325 * Z + (Z - 623.531722222222)
* (Z - 623.531722222222) * 0.859410097557437 + (Z - 623.531722222222)
* (Z - 623.531722222222) * (Z - 623.531722222222) * 0.116897099521817

+ 2.30898218858094 * Y + (Y - 4120320.76712037) * (Y - 4120320.76712037)
* 0.0289065652753111 + (Y - 4120320.76712037) * (Y - 4120320.76712037)
* (Y - 4120320.76712037) * 0.000122300616539063

+ -1.81585992777963 * X + (X - 551230.813768519) * (X - 551230.813768519)
* 0.0288436968560567 + (X - 551230.813768519) * (X - 551230.813768519)
* (X - 551230.813768519) * -0.000120068311574479

# Appendix B
## Regression Formula used to calibrate Trimble® GPS XYZ to Pixel X in the Left Zone

25918464.3649082 + -13.8627267324333 * Z + (Z - 624.015615384615)
* (Z - 624.015615384615) * 0.772230667826512 + (Z -624.015615384615)
* (Z - 624.015615384615) * (Z - 624.015615384615) * 0.119762859942785

+ -5.92595827754575 * Y + (Y - 4120354.15261539) * (Y - 4120354.15261539)
* -0.0937973329703263 + (Y - 4120354.15261539) * (Y - 4120354.15261539)
* (Y - 4120354.15261539) * -0.000858840323752313

+ -2.70764514893634 * X + (X - 551263.725076923) * (X - 551263.725076923)
* 0.0225216836258272 + (X - 551263.725076923) * (X - 551263.725076923)
* (X - 551263.725076923) * -0.000102837635645572

## Regression Formula used to calibrate Trimble® GPS XYZ to Pixel Y in the Left Zone

(-4587386.34397925) + -18.4042747672024 * Z + (Z -624.015615384615)
* (Z - 624.015615384615) * 3.7774985416762 + (Z - 624.015615384615)
* (Z - 624.015615384615) * (Z - 624.015615384615) * 1.56684775268381

+ 1.34884661344953 * Y + (Y - 4120354.15261539) * (Y - 4120354.15261539)
* 0.0405682221336637 + (Y - 4120354.15261539) * (Y - 4120354.15261539)
* (Y - 4120354.15261539) * 0.00058097487771029

+ -1.7386310253344 * X + (X - 551263.725076923) * (X - 551263.725076923)
* 0.0190870028332175 + (X - 551263.725076923) * (X - 551263.725076923)
* (X - 551263.725076923) * -0.000069867453712879

# Appendix C
## Regression Formula used to calibrate Trimble® GPS XYZ to Pixel X in the Upper Zone

24596202.8061441 + 17.0821571345107 * Z + (Z - 621.479787234042)
* (Z - 621.479787234042) * 1.86775357217426 + (Z - 621.479787234042)
* (Z - 621.479787234042) * (Z - 621.479787234042) * -2.40820268669032

+ -5.27289090844702 * Y + (Y - 4120284.80529787) * (Y - 4120284.80529787)
* -0.0307395402808697 + (Y - 4120284.80529787) * (Y - 4120284.80529787)
* (Y - 4120284.80529787) * -0.000158498760564389

+ -5.22499259122168 * X + (X - 551266.56393617) * (X - 551266.56393617)
* 0.0300602990901327 + (X - 551266.56393617) * (X - 551266.56393617)
* (X - 551266.56393617) * -0.00018058511094501

## Regression Formula used to calibrate Trimble® GPS XYZ to Pixel Y in the Upper Zone

(-2265497.53831517) + 1.23561071421368 * Z + (Z - 621.479787234042)
* (Z - 621.479787234042) * -0.812299344054743 + (Z - 621.479787234042)
* (Z - 621.479787234042) * (Z - 621.479787234042) * 0.0880290154506851

+ 0.6652670697114 * Y + (Y - 4120284.80529787) * (Y - 4120284.80529787)
* 0.00652964436172477 + (Y - 4120284.80529787) * (Y - 4120284.80529787)
* (Y - 4120284.80529787) * 0.0000434809097013779

+ -0.86341444857543 * X + (X - 551266.56393617) * (X - 551266.56393617)
* 0.00640689190935397 + (X - 551266.56393617) * (X - 551266.56393617)
* (X - 551266.56393617) * -0.0000291014404628619

# Appendix D
## Regression Formula used to calibrate Trimble® GPS XYZ to Pixel X in the Right Zone

15245198.8063553 + -9.83770572837577 * Z + (Z - 623.678928571429)
* (Z - 623.678928571429) * -0.226653270161887 + (Z -623.678928571429)
* (Z - 623.678928571429) * (Z - 623.678928571429) * 0.0794772209088345

+ -2.51232935000568 * Y + (Y - 4120294.59992857) * (Y - 4120294.59992857)
* -0.0217840178488246 + (Y - 4120294.59992857) * (Y - 4120294.59992857)
* (Y - 4120294.59992857) * -0.000198860612049309

+ -8.86512140841613 * X + (X - 551190.216928571) * (X - 551190.216928571)
* 0.204228991189053 + (X - 551190.216928571) * (X - 551190.216928571)
* (X - 551190.216928571) * -0.0034854938319746

## Regression Formula used to calibrate Trimble® GPS XYZ to Pixel Y in the Right Zone

(-695957.037067474) + -41.0707859388993 * Z + (Z - 623.678928571429)
* (Z - 623.678928571429) * -1.80984244680538 + (Z - 623.678928571429)
* (Z - 623.678928571429) * (Z - 623.678928571429) * 0.968105447006676

+ 0.985162596930589 * Y + (Y - 4120294.59992857) * (Y - 4120294.59992857)
* 0.0395032995739219 + (Y - 4120294.59992857) * (Y - 4120294.59992857)
* (Y - 4120294.59992857) * 0.000311055350827217

+ -6.05451332855243 * X + (X - 551190.216928571) * (X - 551190.216928571)
* 0.0425615650785377 + (X - 551190.216928571) * (X - 551190.216928571)
* (X - 551190.216928571) * 0.00119232193179383

# Appendix E
## Regression Formula used to calibrate Trimble® GPS XYZ to Pixel X in the Lower Zone

82571073.894918 + -7.45046636350764 * Z + (Z - 626.122588235294)
* (Z - 626.122588235294) * 2.28910018430246 + (Z - 626.122588235294)
* (Z - 626.122588235294) * (Z - 626.122588235294) * 2.0405404259716

+ -17.5904773745776 * Y + (Y - 4120368.48873529)* (Y - 4120368.48873529)
* -0.218783210745992 + (Y - 4120368.48873529)* (Y - 4120368.48873529)
* (Y - 4120368.48873529) * -0.00189249045989212

+ -18.2996996801082 * X + (X - 551185.527029412)
* (X - 551185.527029412) * 0.321046430970257 + (X - 551185.527029412)
* (X - 551185.527029412) * (X - 551185.527029412) * -0.00580529963824531

## Regression Formula used to calibrate Trimble® GPS XYZ to Pixel Y in the Lower Zone

(-24816024.011466) + 1.16102728127327 * Z + (Z - 626.122588235294)
* (Z - 626.122588235294) * 2.68153342187984 + (Z - 626.122588235294)
* (Z - 626.122588235294) * (Z - 626.122588235294) * -1.88174933249601

+ 6.95270068892852 * Y + (Y - 4120368.48873529) * (Y - 4120368.48873529)
* 0.111982555909414 + (Y - 4120368.48873529) * (Y - 4120368.48873529)
* (Y - 4120368.48873529) * -0.000318727937373074

+ -6.95173818866818 * X + (X - 551185.527029412) * (X - 551185.527029412)
* 0.139824878660434 + (X - 551185.527029412) * (X - 551185.527029412)
* (X - 551185.527029412) * 0.0001292110099